Cell Tissue Res (2014) 358:857–873
DOI 10.1007/s00441-014-2006-6

REGULAR ARTICLE

# Transplantation of devitalized muscle scaffolds is insufficient for appreciable de novo muscle fiber regeneration after volumetric muscle loss injury

**Koyal Garg · Catherine L. Ward · Christopher R. Rathbone · Benjamin T. Corona**

Received: 19 June 2014 / Accepted: 9 September 2014 / Published online: 10 October 2014


**Abstract** Volumetric muscle loss (VML) is a traumatic and functionally debilitating muscle injury with limited treatment options. Developmental regenerative therapies for the repair of VML typically comprise an ECM scaffold. In this study, we tested if the complete reliance on host cell migration to a devitalized muscle scaffold without myogenic cells is sufficient for de novo muscle fiber regeneration. Devitalized (muscle ECM with no living cells) and, as a positive control, vital minced muscle grafts were transplanted to a VML defect in the tibialis anterior muscle of Lewis rats. Eight weeks post-injury, devitalized grafts did not appreciably promote de novo muscle fiber regeneration within the defect area, and instead remodeled into a fibrotic tissue mass. In contrast, transplantation of vital minced muscle grafts promoted de novo muscle fiber regeneration. Notably, pax7+ cells were absent in remote regions of the defect site repaired with devitalized scaffolds. At 2 weeks post-injury, the devitalized grafts were unable to promote an anti-inflammatory phenotype, while vital grafts appeared to progress to a pro-regenerative inflammatory response. The putative macrophage phenotypes observed in vivo were supported in vitro, in which soluble factors released from vital grafts promoted an M2-like macrophage polarization, whereas devitalized grafts failed to do so. These observations indicate that although the remaining muscle mass serves as a source of myogenic cells in close proximity to the defect site, a devitalized scaffold without myogenic cells is inadequate to appreciably promote de novo muscle fiber regeneration throughout the VML defect.

**Keywords** Vital and devitalized minced muscle graft · Volumetric muscle loss · Skeletal muscle injury and damage · Tissue engineering · Tissue regeneration

## Introduction

Trauma results in upwards of $400 billion yearly in associated medical costs and loss of productivity worldwide, and is a primary contributor to the global burden of disease and injury (Corso et al. 2006). Vehicle accident-related trauma cases routinely present open fracture and/or soft-tissue injury to the lower extremities, and are projected to rank third in disability-adjusted life years (DALYs) lost in 2020 (Vos et al. 2012). Although primarily from high-energy blast trauma, the majority of injuries sustained in recent military conflicts are to the extremities, and often involve severe musculoskeletal injury involving volumetric muscle loss (VML) (Owens et al. 2007, 2008). The high prevalence of this severe musculoskeletal trauma has highlighted VML as a limitation to successful rehabilitation of salvaged limbs and, in turn, has reinvigorated research efforts directed at regenerating a large volume of muscle tissue. Currently, there is no definitive therapy for VML that regenerates or restores the frank loss of muscle mass.

Endogenous mechanisms of mammalian skeletal muscle repair and regeneration are not efficient in replacing lost muscle tissue after penetrating trauma, i.e., de novo muscle fiber regeneration (Corona et al. 2013a; Wu et al. 2012; Mase et al. 2010). This is at odds with the remarkable capacity of

**Disclaimer** The opinions or assertions contained herein are the private views of the author, and are not to be construed as official or as reflecting the views of the Department of the Army or the Department of Defense.

**Electronic supplementary material** The online version of this article (doi:10.1007/s00441-014-2006-6) contains supplementary material, which is available to authorized users.

K. Garg · C. L. Ward · C. R. Rathbone · B. T. Corona (✉)
US Army Institute of Surgical Research Extremity Trauma and Regenerative Medicine, 3698 Chambers Pass Fort Sam, Houston, TX 78234, USA
e-mail: benjamin.t.corona.vol@mail.mil

# Report Documentation Page

*Form Approved*
*OMB No. 0704-0188*



| 1. REPORT DATE | 2. REPORT TYPE | 3. DATES COVERED |
|---|---|---|
| **01 DEC 2014** | **N/A** | **-** |

| 4. TITLE AND SUBTITLE | 5a. CONTRACT NUMBER |
|---|---|
| **Transplantation of devitalized muscle scaffolds is insufficient for appreciable de novo muscle fiber regeneration after volumetric muscle loss injury** | 5b. GRANT NUMBER |
| | 5c. PROGRAM ELEMENT NUMBER |

| 6. AUTHOR(S) | 5d. PROJECT NUMBER |
|---|---|
| **Garg K., Ward C., Rathbone C. R., Corona B. T.,** | 5e. TASK NUMBER |
| | 5f. WORK UNIT NUMBER |

| 7. PERFORMING ORGANIZATION NAME(S) AND ADDRESS(ES) | 8. PERFORMING ORGANIZATION REPORT NUMBER |
|---|---|
| **United States Army Institute of Surgical Research, JBSA Fort Sam Houston, Tx 78234** | |

| 9. SPONSORING/MONITORING AGENCY NAME(S) AND ADDRESS(ES) | 10. SPONSOR/MONITOR'S ACRONYM(S) |
|---|---|
| | 11. SPONSOR/MONITOR'S REPORT NUMBER(S) |

12. DISTRIBUTION/AVAILABILITY STATEMENT
**Approved for public release, distribution unlimited**

13. SUPPLEMENTARY NOTES

14. ABSTRACT

15. SUBJECT TERMS

| 16. SECURITY CLASSIFICATION OF: | | | 17. LIMITATION OF ABSTRACT | 18. NUMBER OF PAGES | 19a. NAME OF RESPONSIBLE PERSON |
|---|---|---|---|---|---|
| a. REPORT | b. ABSTRACT | c. THIS PAGE | | | |
| **unclassified** | **unclassified** | **unclassified** | **UU** | **17** | |

muscle to repair and regenerate following other types of injuries (e.g., eccentric and toxin). VML presents such a challenge because necessary regenerative elements, namely satellite cells and the basal lamina, are physically removed. In effect, there is a void in which there are no remnants of the pre-existing muscle to repair. That is, prolonged functional deficits after VML are primarily due to the frank loss of muscle fibers and their contractile machinery.

An attractive approach for the repair of VML is the transplantation of a myoinductive decellularized scaffold (i.e., an extracellular matrix) that attracts, from the host, the cells required for adult myogenesis. Biological scaffolds are used in a variety of clinical tissue engineering applications (Keane and Badylak 2014) and have been studied in preclinical skeletal muscle VML injury models frequently over the last decade (e.g., Brown et al. 2009; Corona et al. 2013a, 2013b; Gamba et al. 2002; Machingal et al. 2011; Merritt et al. 2010a; Valentin et al. 2010). Signifying the potential emergence of this therapy to clinical practice, transplantation of a porcine-derived xenogeneic scaffold (small intestine submucosa; SIS, or urinary bladder matrix; UBM) to VML in the lower extremities appeared to be tolerated, although the magnitude of muscle fiber regeneration appeared limited (Mase et al. 2010; Sicari et al. 2014). In most preclinical studies, scaffold-mediated de novo muscle fiber regeneration also appears limited or restricted to sites close to the remaining muscle tissue (Corona et al. 2013b; Merritt et al. 2010a; Brown et al. 2012). However, extreme observations of muscle tissue regeneration ranging from *quite remarkable* (Turner et al. 2010) to *absolutely aberrant* (Corona et al. 2013a; Gamba et al. 2002; Turner et al. 2012) have also been reported. There are numerous potential explanations for the variability among studies in observing de novo fiber regeneration following transplantation of biological scaffolds, to include source and preparation (Keane and Badylak 2014). Among these methodological considerations, a fundamental question is also raised as to whether a scaffold devoid of myogenic and other resident stem and progenitor cells is able to orchestrate the complex spatiotemporal events necessary for appreciable muscle fiber regeneration.

The promise of a myoinductive acellular scaffold as a therapy for VML is predicated on the basic works published in the late 1900s, in which transplanted devitalized whole or minced muscle grafts were shown to support de novo skeletal muscle regeneration. For instance, devitalized whole extensor digitorum longus (EDL) muscle was shown to support a low level of muscle fiber regeneration in mice without the exogenous delivery of a myogenic cell source (Morgan et al. 1987). In addition, Schultz et al. (1986) demonstrated that rat EDL muscle devitalized in situ could support muscle fiber regeneration if either a portion of the muscle remained healthy, or if the devitalized area was tethered to an injured adjacent muscle (tibialis anterior (TA) muscle)—a scenario similar to current VML models (Merritt et al. 2010a; Wu et al. 2012). However, when devitalized EDL muscles were not in connection with an injured muscle bed, despite maintaining vascular supply from the host, muscle fiber regeneration was aberrant, suggesting the need for an activated source of nearby myogenic cells to promote regeneration (Schultz et al. 1986). Supporting this notion, Ghins et al. (1984, 1985, 1986), demonstrated that devitalized grafts transplanted after complete triceps surae removal in juvenile rats promoted virtually no muscle fiber regeneration unless supplemented with autologous vital minced grafts or cultured muscle progenitor cells.

Because VML models leave remnants of injured muscle actively regenerating (Corona et al. 2013c), it is therefore plausible that the remaining muscle mass can supply cell populations to a myoinductive scaffold, resulting in de novo muscle fiber regeneration. Herein, we test this hypothesis in a rat TA muscle VML model (Corona et al. 2013a, 2013c) in which transplanted devitalized grafts (devoid of any live resident muscle cells) are in close proximity to the *injured* remaining musculature.

In this study, we have chosen to use devitalized minced muscle grafts because derivations of this scaffold (e.g., decellularized allogeneic or xenogeneic scaffolds) are capable of supporting de novo muscle fiber regeneration in whole muscle ablation models under distinct conditions in which an active myogenic cell source is readily available (Schultz et al. 1986; Ghins et al. 1984). Vital minced muscle grafts were used as a positive control for de novo muscle fiber regeneration in the VML defect. Muscle fiber regeneration and the innate immune response to devitalized and vital minced muscle grafts were investigated in vivo, and macrophage polarization was studied in vitro.

## Methods

*Experimental design* Male Lewis rats with VML were repaired with either devitalized or vital autologous minced muscle grafts. Rats from each treatment group were recovered out to 14 days or 8 weeks post-injury (devitalized and vital; $n=5$ and 6 per group, respectively). At these times, TA muscles were collected for histological and molecular analyses. At 8 weeks only, rats underwent in vivo functional testing of the anterior crural muscles prior to tissue harvest. An additional VML injured no repair group ($n=5$) was included for functional assessment to ascertain therapeutic benefits of devitalized and vital grafts. To further investigate the effect of devitalized and vital grafts on macrophage polarization, in vitro transwell culture assays were performed.

*Animals* This work has been conducted in compliance with the Animal Welfare Act, the implementing Animal Welfare Regulations and in accordance with the principles of the

Guide for the Care and Use of Laboratory Animals. All animal procedures were approved by the United States Army Institute of Surgical Research Institutional Animal Care and Use Committee. Adult male Lewis rats (Harlan Laboratories, Indianapolis, IN, USA) were housed in a vivarium accredited by the Association for Assessment and Accreditation of Laboratory Animal Care International, and provided with food and water ad libitum.

*Surgical creation and treatment of VML injury* The surgical procedure for creating VML in the rat TA muscle was performed as described previously (Wu et al. 2012; Corona et al. 2013a). Using aseptic technique, a surgical defect of ~10 × 7 × 3 mm (length x width x depth) was created in the middle third of the TA muscle in left leg using a scalpel. The excised defect weight approximated 20 % of the estimated TA muscle weight, using a regression equation based on the rat's body weight at the time of surgery, as reported previously (Wu et al. 2012). As per experimental condition, TA muscles were repaired with vital tissue, also referred to as autologous minced muscle grafts, which were created using the piece of TA muscle excised for the VML defect and mincing it into ~1 $mm^3$ fragments. To create devitalized tissue, minced fragments were flash frozen in liquid nitrogen, thawed, and heated for 10 mins at 65 °C. The minced tissue and the devitalized tissue were then placed orthotopically into the fresh wound bed and the fascia was closed using Vicryl suture followed by skin closure. Rats were administered sustained release buprenorphine-HCl, 1.2 mg/kg, SC, 30 minutes before surgery.

*In-vivo tibialis anterior muscle functional testing* TA muscle in vivo mechanical properties were measured in anesthetized rats (isoflurane 1.5–2.0 %) in both legs as previously described (Corona et al. 2013c). Core body temperature was monitored and maintained at ~36–37 °C. A nerve cuff with multistranded stainless steel (Cooner Wire, 632) wire electrodes was implanted immediately before testing in each leg around the peroneal nerve. Legs were tested separately and in randomized order. The foot was strapped using silk surgical tape to a footplate attached to a dual-mode muscle lever system (Aurora Scientific, Inc., Mod. 305b). The knee was secured on either side using a custom-made mounting system, and the knee and ankle were positioned at right angles. Optimal voltage (2–5 V) was set with a series of tetanic contractions (5–10 contractions; 150 Hz, 0.1 ms pulse width, 400 ms train). Then, a skin incision was made at the anterolateral aspect of the ankle, and the distal EDL muscle tendon and extensor hallicus longus (EHL) muscle was isolated and severed above the retinaculum. The TA muscle and tendon, as well as the retinaculum, were undisturbed. Four to five tetani were performed with a 1-minute rest interval to allow for torque stabilization. The contribution of the tenotomized EDL muscle was negligible in this testing system (Corona et al. 2013c). This is likely, because the released EDL muscle was in an extremely shortened position and therefore produced little force upon stimulation (Huijing and Jaspers 2005). TA muscle maximal tetanic isometric torque was determined across a range of stimulation frequencies (100–200 Hz) with at least a 1-minute rest interval (0.1 ms pulse width, 400 ms train). To control for variation in body weight among groups, isometric torque (Nmm) was normalized body weight (kg).

*Scanning electron microscopy* After mincing, autograft tissue (vital or devitalized) was placed in a well-plate and fixed with 2.5 % phosphate-buffered glutaraldehyde (0.1 M pH 7.2–7.4) overnight at 4 °C. The tissue was then washed with phosphate buffered saline (PBS) and dehydrated through a series of alcohol concentrations (50–100 %) before air drying. The tissue was mounted to a specimen stub using double-sided carbon tape. Samples were sputter-coated with gold (108 Auto Sputter Coater, TedPella, Inc, Redding, CA, USA) and then visualized using a Carl Zeiss VP-40 field emission scanning electron microscope (Oberkochen, Germany) operated at a scanning voltage of 2 kV.

*In-vitro cell culture* TA muscle tissue was minced to approximately 1 $mm^3$ pieces. Single autograft pieces (vital and devitalized) were placed in wells of a 48-well tissue culture treated plate coated with collagen (Rat Tail Collagen I, BD Biosciences, 25 $\mu g/cm^2$ in 0.02 M acetic acid). Autograft tissue was cultured in growth medium (DMEM/F12 supplemented with 20 % fetal bovine serum and 1 % penicillin/streptomycin) for up to 14 days at 37 °C and 5 % $CO_2$. On days 1, 4, 7, 11, and 14, plates were washed with PBS and stored at −80 °C. A CyQUANT® cell proliferation assay was performed according to the manufacturer's instructions (Life Technologies™) for each timepoint ($n$=6 wells). Plates were read on a SpectraMax M2 plate reader (Molecular Devices). Background was diminished by subtracting appropriate blank controls that contained growth media in collagen-coated wells. Resulting nucleic acid concentrations were obtained per well by correlating to a standard curve. Additionally, cells emanating from vital minced grafts were also cultured on laminin-111 (Invitrogen) coated 48 well plates. The myogenic cells on collagen and laminin coated well plates were stained after 14 days of culture with desmin (Sigma) and Alexa Fluor 488 or 594 (Invitrogen) as described previously (Corona et al. 2013c).

*In-vitro macrophage (MΦ) phenotype experiment* Adult male Lewis rats were euthanized, the bone marrow was isolated from the femurs and tibias, and the red blood cells were lysed. The harvested bone marrow was cultured in complete RPMI (with 1 % penicillin and streptomycin, L-glutamine, HEPES, sodium pyruvate, 10 % FBS, and 30 ng/ml recombinant rat MΦ-colony stimulating factor (rM-CSF)). The culture

was allowed to go on for 7 days in the presence of rM-CSF (30 ng/ml). After maturation, the bone marrow derived macrophages (BMMΦ) were divided into three different groups and stimulated for 48 h in the presence of either rat IL-4 and IL-13 (Peprotech, 20 ng/ml each) to polarize BMMΦ to an M2 phenotype or rat INF-γ (Peprotech, 20 ng/ml) and LPS (Sigma-Aldrich L6529, 100 ng/ml) to polarize the BMMΦ to an M1 phenotype. Untreated BMMΦs constituted the naïve group (M0s). The minced graft and devitalized graft pieces were put in a 3 μm pore transwell in a 24-well plate with the BMMΦ (M0, M1 and M2) cultured on the well plate on the bottom for 1 or 4 days ($n$=3/group/time).

*Histological & immunohistochemistry analysis* TA muscles were embedded in a talcum-based gel and frozen in 2-methylbutane (Fisher Scientific) super-cooled in liquid nitrogen using standard methodology reported previously (Corona et al. 2013a). Frozen cross-sections (8 μm) were cut from the middle third of the TA muscle in the area where the original surgical defect was made. Immunofluorescence stained tissue sections were probed for collagen I (1:500, Millipore AB755P), sarcomeric myosin (MF20: 1:10, Hybridoma Bank), laminin (1:200, Abcam AB11575), CD68 (1:50, AbD Serotec MCA341R), Pax 7 (1:500, Abcam ab34360), Sca-1 (1:500, Millipore, AB4336), cellular membranes (wheat germ agglutinin, WG; 1:1000, Invitrogen) and nuclei (DAPI; 1:100, Invitrogen). Corresponding Alexa Flour® 488 and 596 labeled secondary antibodies (1:200–1:500), Invitrogen) were incubated at room temperature for 1 h. Qualitative assessments of immunostained sections were made by observing three sections (separated by no less than 160 μm) from 3–5 muscles per time point per group. Additionally, the area fraction of collagen 1 and myosin in the defect area of dual-probed sections was quantified in non-overlapping images using ImageJ (NIH). RGB channels were separated and then thresholded to remove background. Sections from devitalized, and minced graft-repaired VML injured muscles were also stained with hematoxylin and eosin (H&E).

*RT-PCR* RNA was isolated from snap-frozen cross-sections of TA muscle that was comprised of the defect area and the remaining muscle mass (50–100 mg). RNA was extracted using Trizol LS reagent (Invitrogen), and purified using RNeasy mini kit (Qiagen). The yield of RNA was quantified using a NanoDrop spectrometer (NanoDrop Technologies Inc.) and optical density $(OD)_{260/280}$ ratios were determined. RNA (500 ng) was reverse-transcribed into cDNA using the Super-Script® III first-strand synthesis kit (Invitrogen). The primer sets used in the study are listed in Table 1. All primer sets have been synthesized by Sigma-Aldrich DNA oligos design tool. Aliquots (2 μL) of cDNA were amplified with 200nM forward/reverse primers, SYBR GreenER (Invitrogen) in triplicate using a Bio-Rad CFX96 thermal cycler system (Bio-Rad). Nontemplate control and no reverse transcriptase controls were run for each reaction. Gene expression was normalized to 18S (housekeeping gene) to determine the ΔCT value. Expression levels for each mRNA transcript were determined by the $2^{-\Delta\Delta CT}$ method by normalizing each group (devitalized or vital graft) to its contralateral control ($n$=3–6 per group).

*Western blot* The soluble protein fraction of cross-sections that comprised the defect area and remaining muscle mass of TA muscles was extracted as described previously (Corona et al. 2013c). The protein isolated from these tissues ($n$=5/group) was probed for Collagen 1 (Abcam, ab90395) and Pax 7 (Abcam, ab34360) via Western blot at 2 or 8 weeks post–injury. The cell lysates ($n$=3/group) from BMMΦ were analyzed for Arginase1 and iNOS expression by western blot on Day 1 and 4 of culture. Protein concentrations were determined with the Pierce BCA protein assay kit (Thermo Scientific). Proteins were resolved by SDS-PAGE using total protein from cell lysates (10 μg) and tissue homogenates (20 μg, Col1; 40 μg Pax7) on 4–20 % Tris-glycine gels (Bio-Rad). Transfer was made onto nitrocellulose membranes subsequently blocked for 1 h at room temperature in Tris-buffered saline containing 0.05 % (*v/v*) Tween 20 (TBST) and 5 % (*w/v*) nonfat dried milk. Membranes were then incubated overnight at 4 °C in TBST containing 5 % (w/v) bovine serum albumin and primary antibody diluted 1:1000. Membranes were rinsed 6 times in TBST, and then incubated at room temperature for 1 h in TBST and 5 % milk containing peroxidase-conjugated goat anti-rabbit secondary antibody diluted 1:2000. Membranes were rinsed 6 times in TBST before exposure to ECL Reagents (Invitrogen). The membranes were then imaged using the Odyssey® Fc system (LI-COR Biosciences).

### Statistics

Dependent variables were analyzed using one and two-way ANOVAs or independent samples $t$-tests. Post hoc means comparisons testing was performed when a significant ANOVA was observed. Alpha was set at 0.05. Values are listed as means ± SE. Statistical testing was performed with Prism 6 for Mac (Graphpad, La Jolla, CA, USA).

## Results

### In-vitro analysis of vital and devitalized minced grafts

TA muscle was minced into ~1 $mm^3$ pieces, and both the devitalized and vital grafts were analyzed by SEM (Fig. 1 a, b). The images show lysed cell debris in the devitalized grafts,

**Table 1** Nucleotide sequence for primers used for quantitative RT-PCR

| | Forward sequence | Reverse sequence | Amplicon length, bp |
|---|---|---|---|
| ARG1 | 5′-GTGAAGAACCCACGGTCTGT-3′ | 5′-GTGAGCATCCACCCAAATG-3′ | 180 |
| CCR7 | 5′-GCTCTCCTGGTCATTTTCCA-3′ | 5′-AAGCACACCGACTCATACAGG-3′ | 107 |
| CD163 | 5′-TCATTTCGAAGAAGCCCAAG-3′ | 5′-CTCCGTGTTTCACTTCCACA-3′ | 101 |
| eMHC | 5′-TGGAGGACCAAATATGAGACG-3′ | 5′-CACCATCAAGTCCTCCACCT-3′ | 180 |
| FIZZ1 | 5′-CATCTGCGTCTTCCTTCTCC-3′ | 5′-GAGGCCCATTTGCTCATAGA-3′ | 171 |
| IL-4 | 5′-TGATGTACCTCCGTGCTTGA-3′ | 5′-AGGACATGGAAGTGCAGGAC-3′ | 197 |
| IL-10 | 5′-CCCAGAAATCAAGGAGCATT-3′ | 5′-GCTCCACTGCCTTGCTTTTA-3′ | 116 |
| IL-12 | 5′-GCTTCTTCATCAGGGACATCA-3′ | 5′-TTTTCTTTCTTGCGCTGGAT-3′ | 169 |
| MRC1 | 5′-CAAAACAAAGGGACGTTTCG-3′ | 5′-CCTGCCACTCCAGTTTTCAT-3′ | 116 |
| Myogenin | 5′-CTACAGGCCTTGCTCAGCTC-3′ | 5′-GTTGGGACCAAACTCCAGTG-3′ | 153 |
| Pax7 | 5′-GCAGTCGGACCACATTCAC-3′ | 5′-CGCACGACGGTTACTGAAC-3′ | 155 |
| TGF-β1 | 5′-GTCAGACATTCGGGAAGCA-3′ | 5′-CCAAGGTAACGCCAGGAAT-3′ | 138 |
| TNF-α | 5′-ACTCGAGTGACAAGCCCGTA-3′ | 5′-CCTTGTCCCTTGAAGAGAACC-3′ | 184 |
| VEGF | 5′-TGAGACCCTGGTGGACATCT-3′ | 5′-TGGCTTTGGTGAGGTTTGAT-3′ | 180 |
| 18S | 5′-GGCCCGAAGCGTTTACTT-3′ | 5′-ACCTCTAGCGGCGCAATAC-3′ | 173 |

and bundles of muscle fibers in the vital graft. Both of the grafts were also cultured on collagen-coated dishes for 14 days. The proliferative capacity of cells emanating from the grafts was quantified, and showed a continued increase in the nucleic acid content from day 1 to day 14 (Fig. 1c) for vital but not devitalized grafts. Vital grafts cultured on laminin and collagen for 14 days demonstrated the development of desmin$^+$ multi-nucleated myotubes and presence of desmin$^-$ cells (Fig. S2 in electronic supplementary material), indicating a heterogenous population of stem and progenitor cells capable of myogenic differentiation emanating from the vital grafts.

## Prolonged response after VML (8 weeks post-injury)

*Remodeling of the defect area and remaining muscle mass* To determine the capacity of devitalized minced grafts to promote de novo fiber regeneration in a VML defect, grafts were transplanted and allowed to regenerate over the following 8 weeks, a time period sufficient for muscle regeneration in this model (Corona et al. 2013c). Representative images of TA muscle cross sections from the devitalized and vital repaired groups 8 weeks post-injury are presented in Fig. 2 a–c. Little to no muscle fiber regeneration (myosin$^+$ fibers) occurred in the defect area repaired with devitalized minced grafts. Instead, there was an increased collagen 1 presence in the defect site. In contrast, the muscles repaired with the vital minced grafts demonstrated substantial regeneration of myosin$^+$ muscle fibers within the defect area. H&E-stained sections showed that regenerating fibers had centrally located nuclei, and inflammatory cell infiltrates indicating ongoing remodeling events. However, the orientation of the regenerated muscle fibers was not always in line with the fibers in the adjacent remaining muscle mass. The area fraction of myosin was significantly lower in devitalized than vital grafts (Fig. 2d), and the area fraction of collagen 1 in the defect was similar between groups (Fig. 2e). Little satellite cell (Pax7+) presence was observed in the defect area of devitalized grafts, in contrast to vital grafts (Fig. 2c). Reflecting the immunohistological findings in the defect area, the protein content of Pax7 was lower in the devitalized than the vital graft repaired muscles (Fig. 2f) and the protein content of collagen 1 was higher in the devitalized than the vital graft repaired muscles (Fig. S1)

## TA muscle weight and functional capacity

There were no differences in contralateral control TA or EDL muscle weights. The weight of the tissue excised to create the VML defect was similar among groups (Table 2). Devitalized and vital graft repair restored TA muscle weight to similar values as their contralateral control muscles, although vital graft repaired muscles weighed significantly more (+12 %) than those repaired with devitalized grafts ($p<0.05$). In all injured legs, EDL muscle weight was significantly greater than respective contralateral control muscles (+21 %), suggesting compensatory hypertrophy occured.

Maximal tetanic isometric TA muscle torque was assessed 8 weeks post-injury in vivo. Contralateral, non-repaired, and devitalized and vital minced graft repaired VML-injured muscles were assessed. No differences were observed among contralateral control muscles in the groups tested (Fig. 3; Table 2). The VML-injured legs in all groups generated significantly less torque than their respective contralateral controls (e.g., no repair −36.2 %). Compared to VML injured non-repaired muscles, there were significant improvements with devitalized (+17 %) and vital graft (+34 %) repair; the

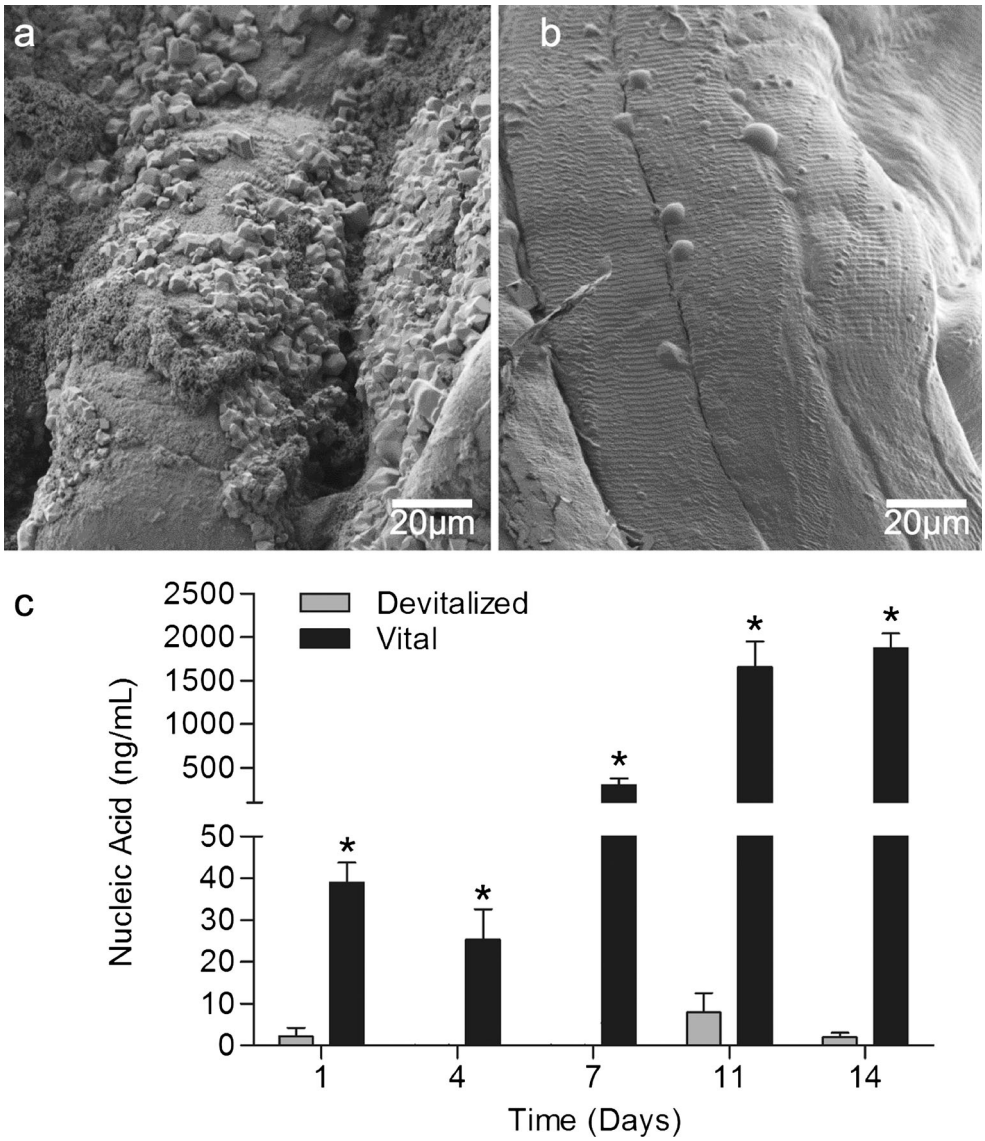


**Fig. 1** Devitalized and vital muscle graft characterization in vitro. Scanning electron microscopy was performed to illustrate the gross structure of the (**a**) devitalized and (**b**) minced muscle grafts. **c** Devitalized and minced muscle grafts were cultured in vitro to demonstrate the proliferative capacity of the resident progenitor cells in the minced muscle. Proliferation was analyzed by measuring the nucleic acid content over 14 days in culture. Values are means ± SEM. *, $P<0.05$

vital graft group produced significantly greater torque than the devitalized graft group (+15 %).

Early response after VML (2 weeks post-injury)

*Tissue presence in the defect* After observing that devitalized grafts did not notably promote de novo fiber regeneration 8 weeks post-injury, observations of the acute response to the devitalized and vital grafts were made to broadly identify potential mechanisms for their regenerative deficiency. Two weeks post-injury, immunohistological analyses of tissue regeneration were performed (Fig. 4). The defect site repaired with devitalized grafts exhibited little evidence of muscle fiber regeneration, marked by a few clusters of myosin-positive fibers in close proximity to the remaining muscle mass (i.e., *the interface*). In contrast, vital minced grafts presented small myosin positive fibers throughout the defect area (Fig. 4d)—the area fraction of myosin was significantly lower in devitalized than in vital grafts (Fig. 4m). Connective tissue (laminin$^+$ (Fig. 4a–f) and collagen 1$^+$ (Fig. 4g–l)) was abundant in the defect area of both types of graft-repaired muscles, and the area fraction of collagen 1 in the defect was similar between groups (Fig. 4n).

*Cellular presence in the defect* The general identity of cell types within the defect of both types of graft-repaired muscle was also investigated immunohistologically 2 weeks post-transplantation. Reflecting the spatial orientation of muscle fiber regeneration with devitalized and vital grafts, pax7$^+$ cells were only observed at the interface in devitalized muscle grafts, but throughout the defect area in vital graft-repaired muscles (Fig. 5a). Reflecting the immunohistological findings in the defect area, the protein content of Pax7 was lesser in the devitalized than the vital graft repaired

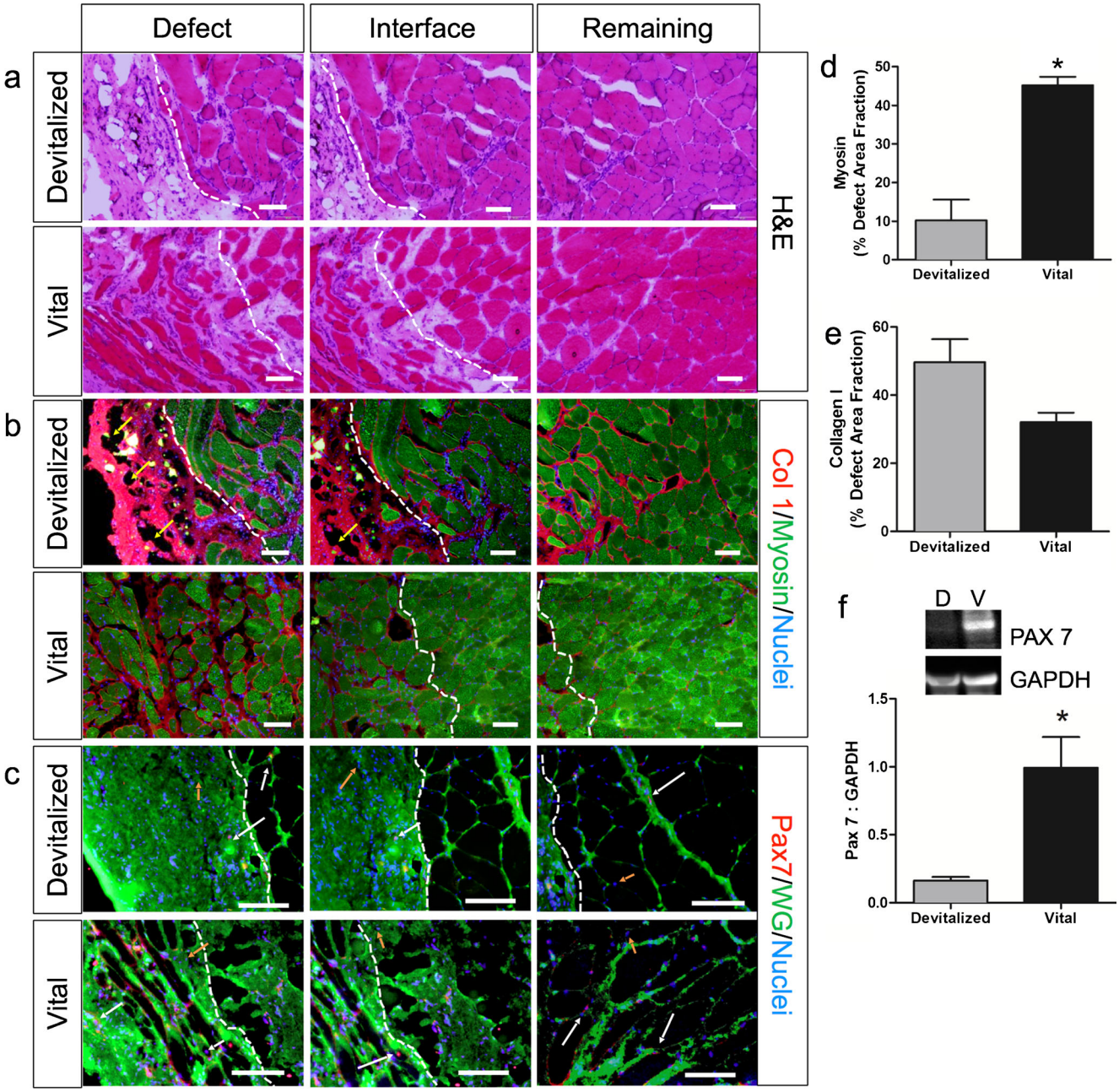


**Fig. 2** Devitalized grafts do not promote appreciable de novo skeletal muscle fiber regeneration in VML-injured TA muscle. Representative images from the cross-sectional area of the defect, interface, and the remaining muscle mass 8 weeks post-injury are shown. **a** Hematoxylin and eosin stained section of the defect area shows chronic injury in the devitalized muscle graft, as compared to the vital minced muscle graft, which shows de novo skeletal muscle fiber regeneration. **b** TA muscle cross sections were probed for myosin and collagen 1 (*yellow arrows* denote the void space in the devitalized graft) and (**c**) Pax7 and wheat germ agglutinin (*white arrows* show examples of positively stained cells, and *orange arrows* show unstained nuclei). The defect area was analyzed quantitatively using Image J (**d** and **e**) for myogenesis (myosin, MF20), and extracellular matrix deposition (collagen 1). Protein isolated from these tissues was probed for (**f**) Pax 7 by Western blot. The protein levels were normalized to GAPDH. Significantly increased Pax 7 content was observed in the vital grafts compared to the devitalized grafts. *Scale bars* 100 μm. Values are means±SEM, * $P<0.05$

muscles (Fig. 5d). Stem cell antigen expressing cells [Sca-1$^+$, (Fig. 5b)] were observed in the defect site of both grafts, although qualitatively to a greater extent in devitalized graft-repaired muscle. Evidence of vascularization (vWF$^+$ cells) was observed at the interface and in the defect region for both grafts, suggesting the arrival of the infiltrating cells may have migrated from the systemic or local environment.

*Myogenic gene expression in graft-repaired TA muscle* Pax7, myogenin, and embryonic MHC expression in muscles repaired with devitalized or vital grafts were analyzed to further

**Table 2** Lewis rat body and muscle morphological and functional characteristics

| | No repair | | Devitalized | | Vital | | ANOVA (*P* value) |
|---|---|---|---|---|---|---|---|
| | Contralateral | Injured | Contralateral | Injured | Contralateral | Injured | |
| Sample size | 5 | 5 | 6 | | | | |
| Defect size (mg) | 108±2 | 114±6 | 105±4 | 0.002 | | | |
| Body weight (g) | 416.6±6.9 | 426.4±1.7 | 395.3±5.2*† | 0.002 | | | |
| TA muscle wt (mg) | 693±20 | 554±20# | 669±15 | 625±22* | 682±26 | 703±41*† | < 0.001 |
| EDL muscle wt (mg) | 170±4 | 208±7# | 175±4 | 199±3# | 169±5 | 216±4# | < 0.001[a] |
| *Vivo TA muscle maximal isometric tetanic torque* | | | | | | | |
| Nmm/kg body wt | 62.5±2.4 | 39.9±1.9# | 61.8±0.8 | 46.5±1.0#* | 64.3±3.5 | 53.5±2.8#*† | < 0.001 |
| % deficit | 36.2±1.1 | 24.7±1.8* | 16.4±2.5*† | < 0.001 | | | |

characterize the myogenic response in the tissue 2 weeks post-injury. For all myogenic genes, expression in the devitalized group was significantly lesser than that of the vital group (Fig. 5g). Also, the myogenic response in the devitalized-repaired muscles was low, as only myogenin exhibited an ~2-fold change compared to uninjured contralateral muscle.

*Inflammatory response 2 weeks after graft-repair* Because muscle regeneration involves coordination with the innate immune response, the macrophage ($CD68^+$) invasion in the defect area was characterized—at this time, devitalized grafts presented a significantly greater macrophage content per area than vital grafts (Fig. 6a,b). Additionally, gene expression of inflammatory markers was also analyzed in muscles repaired with each type of graft. Pro-inflammatory markers such as CCR7 and CD86 were similarly upregulated in both groups, with the exception of tumor necrosis factor-alpha (TNF-α) and interleukin-12 (IL-12), which were significantly higher in the vital minced muscle graft group (Fig. 6c–f). The expression of anti-inflammatory markers such as CD163IL-4, transforming growth factor beta (TGF-β1) vascular endothelial growth factor (VEGF), found in inflammatory zone 1 (Fizz1), and IL-10 was significantly higher in the vital minced muscle graft repaired group, with the exception of mannose receptor (MRC1) and arginase 1 which were upregulated similarly in both groups (Fig. 6g-n).

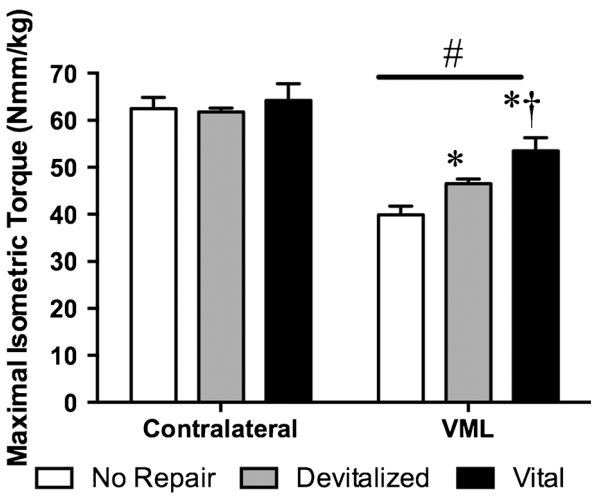


**Fig. 3** Devitalized and vital minced muscle grafts improve in vivo TA muscle torque 8 weeks post-injury. Maximal isometric torque presented for contralateral and injured legs of the devitalized and vital minced grafts-repaired groups. Values are means ± SEM. #, VML<Contralateral; within VML: *, ≠ No Repair, †, ≠ Devitalized; $P<0.05$

*In-vitro macrophage polarization* To elucidate the impact of trophic factors released from devitalized and vital grafts specifically on macrophage polarization, an in vitro macrophage culture system was used (Garg et al. 2013). Naïve macrophages and pre-polarized M1 and M2 macrophages were cultured with devitalized and vital minced muscle grafts in a transwell system for 4 days. On day 1 after culture (Fig. 7a–c), it was observed that naïve macrophages (M0) expressed no Arginase 1 (an M2-like marker). However, statistically similar levels of iNOS (an M1-like marker) were detected from both devitalized and vital minced muscle grafts. Pre-polarized M1 macrophages showed a mixed response of both Arginase 1 and iNOS, as has been shown previously (Garg et al. 2013; Munder et al. 1998, 1999). The pre-polarized M2 macrophages expressed similar levels of Arginase 1, but iNOS was only detected in the vital minced muscle grafts.

On day 4 of culture (Fig. 7d–e), vital minced grafts induced arginase expression in unstimulated naïve macrophages (M0) and further increased arginase expression in pre-polarized M1 and M2 macrophages. Culture with devitalized grafts failed to induce arginase expression in M0 macrophages and reduced arginase expression in pre-polarized M2 macrophages by day 4. The iNOS expression was completely abolished by day 4 in all macrophages (M0, M1, and M2). Collectively, vital minced muscle grafts induced a mixed M1 and M2 response in macrophages on day 1, which was completely replaced by a strong M2 response by day 4.

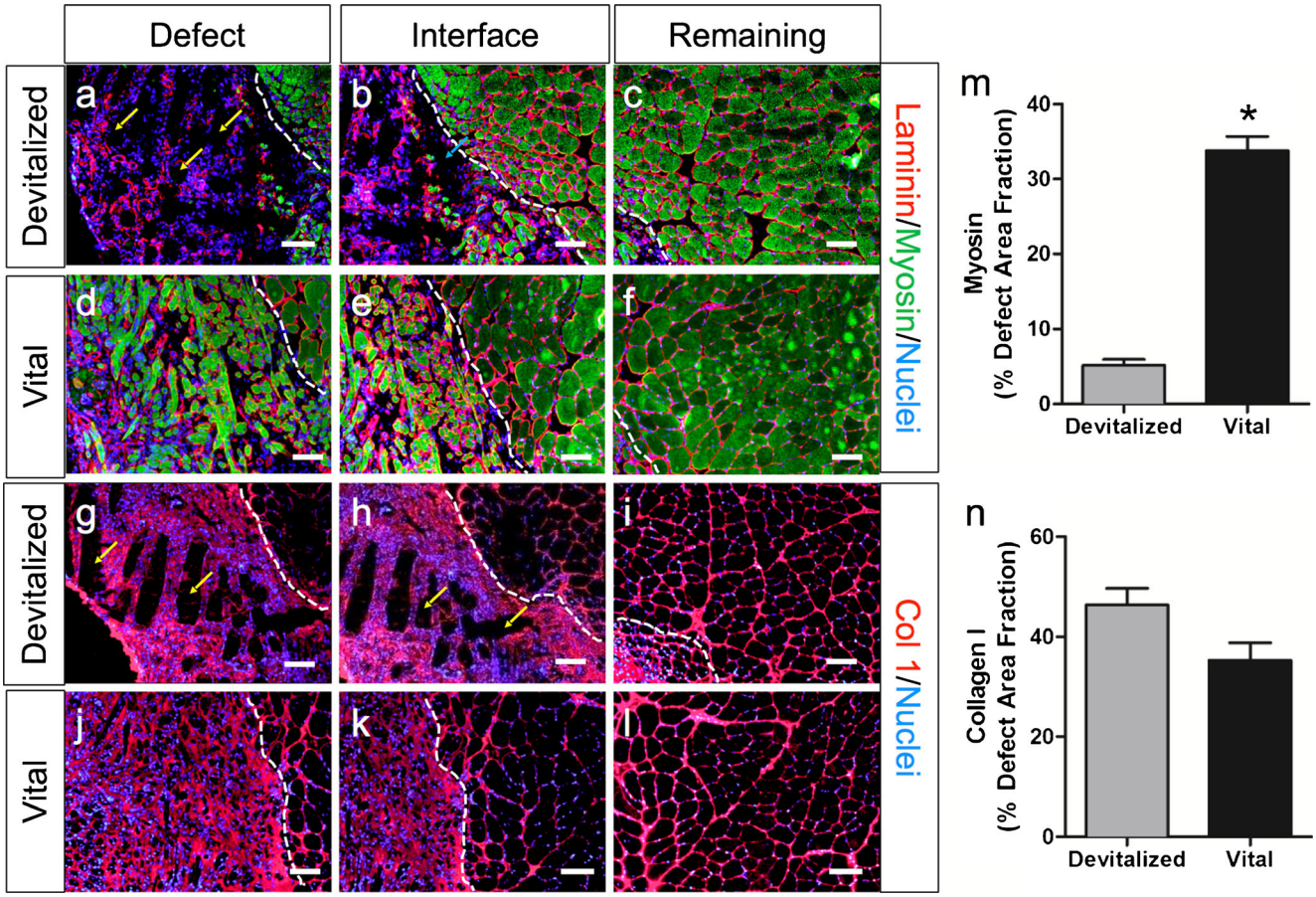


**Fig. 4** Characterization of the tissue deposition in VML injured TA muscles following devitalized and vital minced graft transplantation. The cross-sectional area of the defect, interface, and the remaining muscle mass of TA muscles harvested 2 weeks post-injury is presented. Defect area was analyzed qualitatively using immunohistological staining (**a**–**l**) and quantitatively using Image J (**m** and **n**) for myogenesis (myosin, MF20), and extracellular matrix deposition (collagen 1). *Yellow arrows* denote the void space in the devitalized graft. Only regenerated tissue area within the defect area was included for quantitative analysis. *Scale bar* 100 μm) Values are means±SEM; *, $P<0.05$

## Discussion

Skeletal muscle is endowed with a remarkable capacity to regenerate in cases of physical trauma involving minimal loss of tissue. However, with VML injury a critical mass of muscle is lost that the regenerative capacity of the remaining muscle mass is unable to regenerate or compensate for functionally (Machingal et al. 2011; Merritt et al. 2010b; Grogan and Hsu 2011). Several approaches for the repair of VML have been reported in the literature (e.g., Brown et al. 2009, 2012; Corona et al. 2012, 2013a, c; Rossi et al. 2011). From a regulatory and surgical standpoint, the simple transplantation of a commercially available scaffold is advantageous. However, this approach may be limited in capacity to regenerate muscle tissue de novo in areas remote from the remaining muscle tissue. In the current study, this potential limitation was tested by transplanting devitalized minced muscle grafts into a VML defect that was surrounded by muscle tissue and fascia, which is likely conducive to cell migration and de novo muscle fiber regeneration (Schultz et al. 1985, 1986). Eight weeks post-injury, devitalized grafts failed to appreciably promote de novo muscle fiber regeneration (Fig. 2a,b,d) in regions not directly adjacent to the remaining muscle mass. As a positive control, vital minced grafts promoted de novo fiber regeneration throughout the defect area, as previously reported (Corona et al. 2013c). These findings therefore suggest that an acellular scaffold may be an effective myoconductive therapy for VML when in close proximity to damaged (*activated*) muscle tissue.

The limited de novo muscle fiber regeneration promoted by devitalized grafts was unexpected. Previously, devitalized grafts were shown not to support appreciable myogenesis when the *entire muscle* was devitalized (Schultz et al. 1986; Ghins et al. 1984), even if the devitalized muscle was left intact with the host vasculature (Schultz et al. 1986). However, Ghins et al. (1985, 1986) demonstrated that devitalized grafts have the capacity to support muscle fiber regeneration with co-transplantation of isolated muscle progenitor cells or vital minced grafts in rats. Moreover, in conditions in which damaged muscle tissue is in apposition to devitalized grafts, host myogenic cells can migrate to and partially re-establish the muscle (Schultz et al. 1986). The

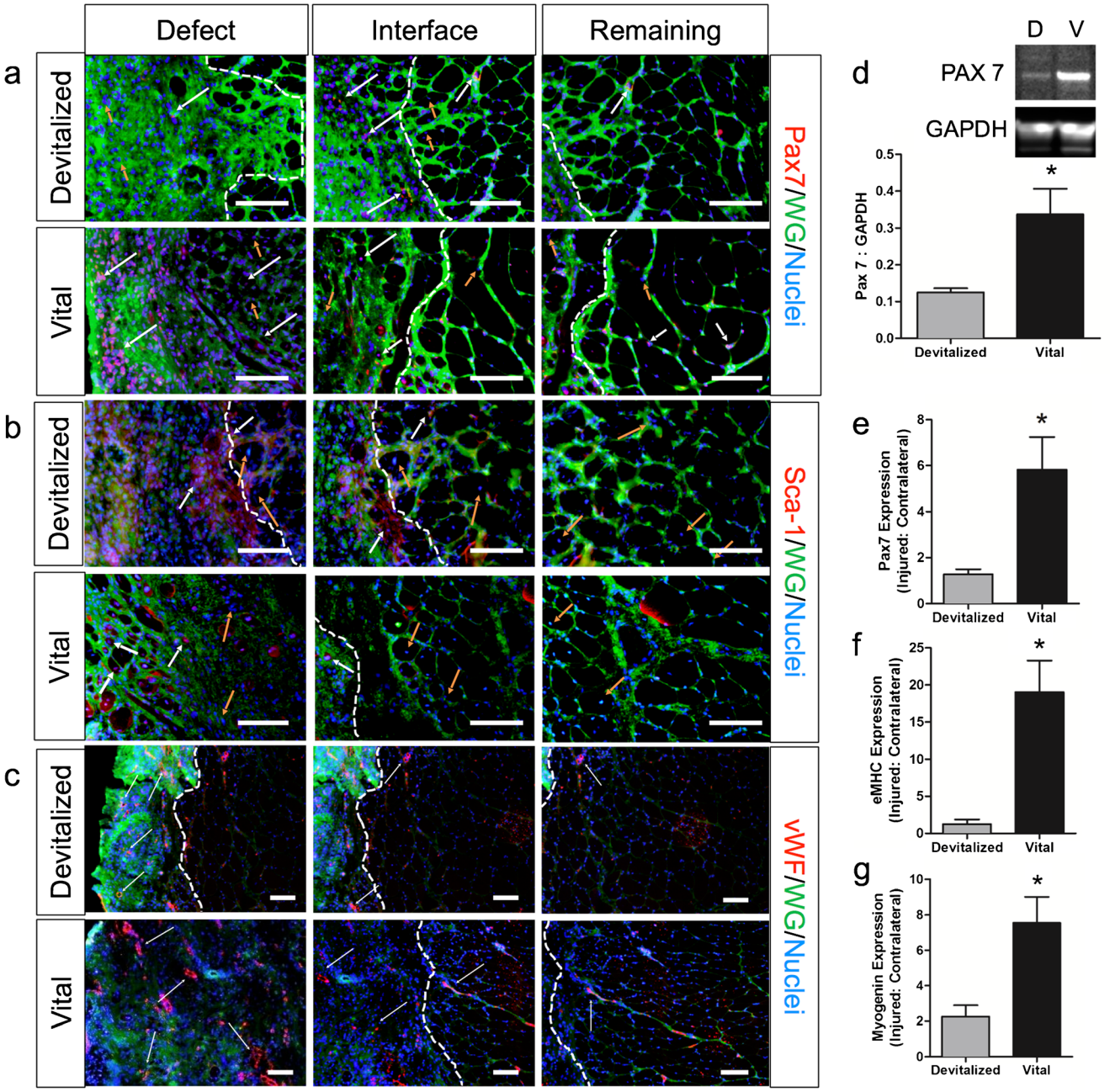


**Fig. 5** The regenerative response of VML-injured TA muscles following devitalized and vital minced graft transplantation. The cross-sectional area of the defect, interface and the remaining muscle mass of TA muscles harvested 2 weeks post-injury is shown. Defect area was analyzed using immunohistological staining for (**a**) satellite cell presence by Pax7 and (**b**) stem cell antigen expressing cells using Sca-1. **c** Vascularization using von Willebrand Factor (vWF). Protein isolated from these tissues was probed for Pax 7 by Western blot (**d**). The protein levels were normalized to GAPDH. Significantly increased Pax 7 content was observed in the vital grafts compared to the devitalized grafts. Tissue samples comprised of the defect area and the remaining muscle mass were assayed for (**e**–**g**) myogenic [Pax 7, embryonic myosin heavy chain (eMHC) and Myogenin] gene expression. *Scale bar* 100 μm) *White arrows* show examples of positively stained cells or vessels, and *orange arrows* show unstained nuclei. Values are means±SEM; *, $P<0.05$

current study was performed in a ~10 × 7 × 3 mm VML defect in the middle third of the TA muscle, surrounded on five sides by remaining tissue that had been damaged during surgery and one side by fascia. Therefore, there was probably an ample repository of activated satellite cells (and other stem cells) to migrate to the devitalized grafts. Furthermore, up to at least 2 weeks post-injury the defect area contained laminin$^{+}$ remnants of the basal lamina of the devitalized tissue (Fig. 4), suggesting an optimal substrate for satellite cell migration within the defect (Siegel et al. 2009). Similar findings

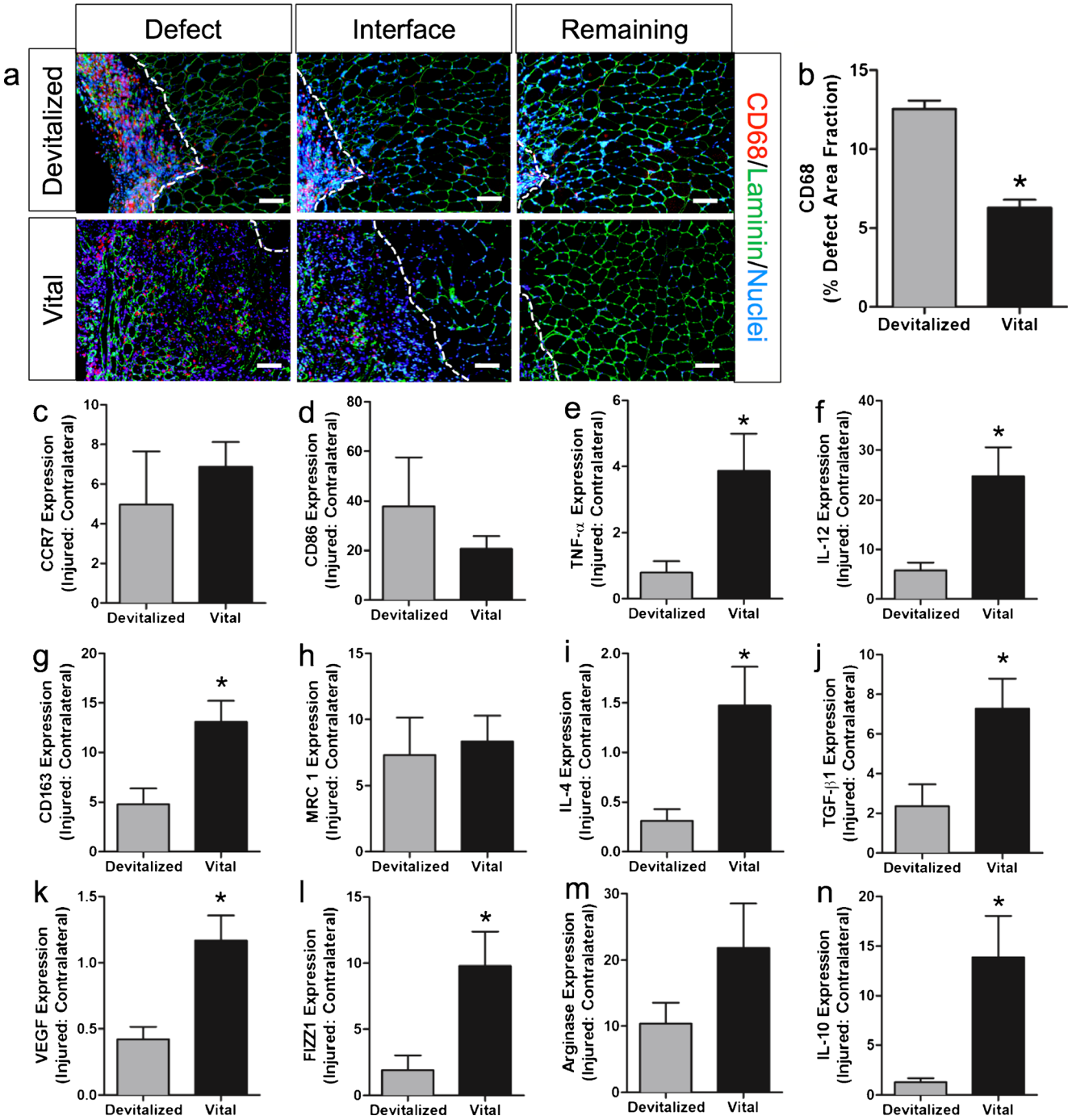


**Fig. 6** The pro- and anti-inflammatory response of VML injured TA muscles following devitalized and vital minced graft transplantation. The cross-sectional area of the defect, interface, and the remaining muscle mass of TA muscles harvested 2 weeks post-injury is presented. Defect area was analyzed using immunohistological staining for (**a**) inflammation using a pan macrophage marker, CD68 and quantitatively using Image J (**b**). Tissue samples comprised of the defect area and the remaining muscle mass were assayed for: (**c**–**f**) Pro-inflammatory (M1-like) markers [CCR7, CD86, tumor necrosis factor alpha (TNF-α) and interleukin-12 (IL-12)], (**g**–**n**) Anti-inflammatory (M2-like) markers [CD163, mannose receptor (MRC1), IL-4, transforming growth factor beta 1 (TGF-β1) and vascular endothelial growth factor (VEGF), found in inflammatory zone 1 (FIZZ1), Arginase 1 and IL-10] gene expression. *Scale bar* 100 μm). Values are means ± SEM; *, $P<0.05$

that muscle regeneration is confined to within a close proximity of the remaining muscle has been demonstrated for decellularized scaffolds derived from muscle (laminin$^{+}$; Corona et al. 2013a; Wolf et al. 2012) and SIS (laminin$^{-}$; Wolf et al. 2012), suggesting that the primary limitation to this approach may not be substrate-specific.

It should be noted that devitalized and decellularized scaffolds are similar yet different in some key aspects. The

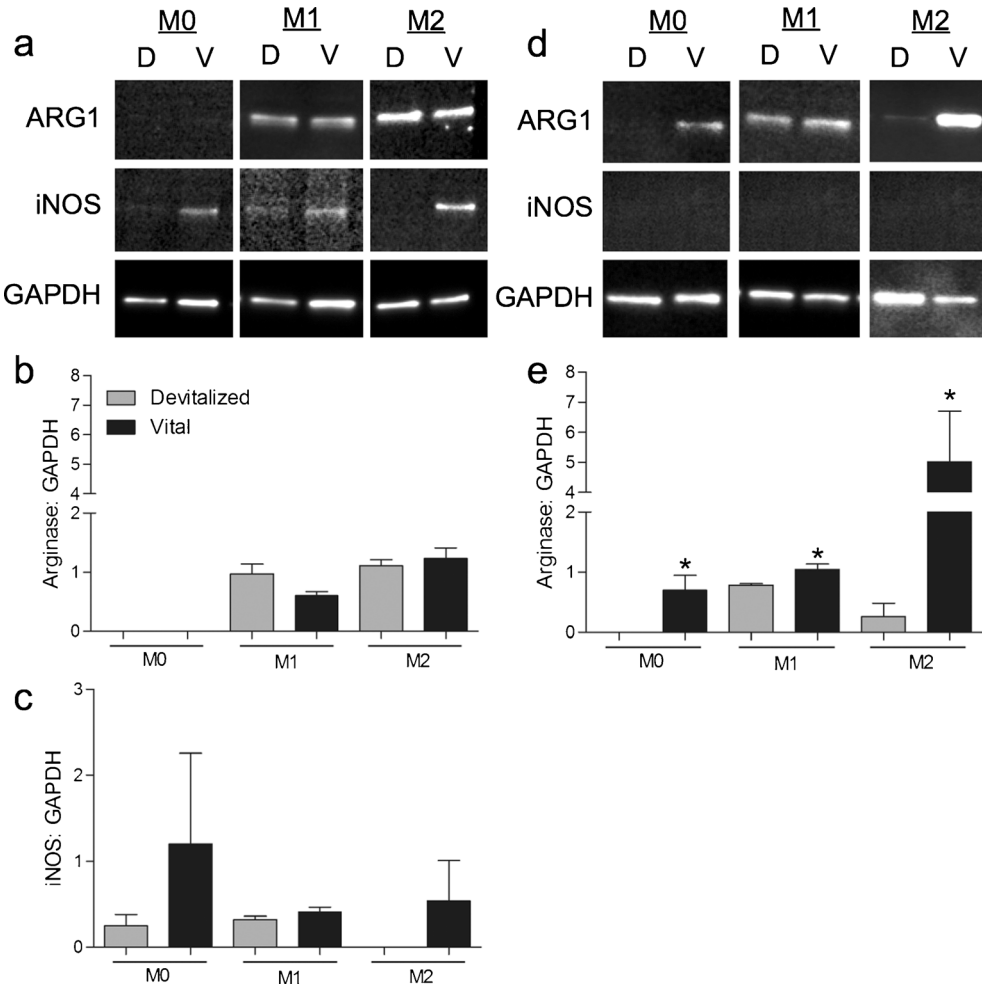


**Fig. 7** Characterization of the macrophage response to devitalized and vital grafts in vitro. Rat bone marrow derived macrophages were cultured in vitro under naïve (M0), pre-polarized M1 and M2 conditions with devitalized and vital grafts in a transwell system for 4 days. **a** The protein isolated from macrophages on day 1 of culture was analyzed for Arginase 1 (Arg1) and iNOS by western blot. **b**, **c** The levels of Arg1 and iNOS were normalized to GAPDH. No significant differences were noted. Vital minced muscle grafts promoted an M2-like phenotype of macrophages in vitro on day 4. **d** The protein was isolated from macrophages on day 4 of culture was analyzed for Arginase 1 (Arg1) and iNOS by western blot. No iNOS expression was detected. **e** The levels of Arg1 were normalized to GAPDH. Arg1 expression was found to be significantly higher in M0, pre-polarized M1, and pre-polarized M2 macrophages on day 4 of culture. Values are means ± SEM; *, $P<0.05$

devitalization procedure has previously been reported to destroy all of the cellular content of the muscle and enzymatic activity; however, cellular debris and DNA fragments may remain (Ghins et al. 1984). The devitalized and vital scaffolds used in the study are autologous, and therefore the cellular remnants (e.g., DNA) in the scaffold carry minimum risk of adverse immune reactions or disease transmission, unlike allogeneic and xenogeneic decellularized scaffolds (Zheng et al. 2005). Importantly, the DNA remnants of the transplanted autologous vital grafts and devitalized scaffolds used herein would elicit similar endogenous responses from the host tissue, allowing for direct comparisons of muscle regeneration (Lu et al. 2011; Seif-Naraghi et al. 2010). The ECM structure of the devitalized scaffolds is expected to remain fairly intact, as the denaturation temperature range of collagen (70–85°C) reported in the literature is well above the temperature (65°C) used in the preparation of the devitalized scaffolds (Lee et al. 1995; Miles and Ghelashvili 1999). In addition, the immunohistological staining clearly shows collagen$^+$ (Fig. 2b, 4g) and laminin$^+$ (Figs. 4a, 6a) structures in the devitalized scaffolds. Therefore, minimum alterations in the ECM structure are expected with devitalized scaffolds, as previously reported for detergent and enzyme-decellularized scaffolds (Williams et al. 2009; Liao et al. 2008; Schenke-Layland et al. 2003). That being said, acellular scaffolds derived from intricate decellularization processes may react differently from the devitalized scaffold used in this study, and therefore caution should be used in making direct comparisons between devitalized and decellularized scaffolds.

A central thesis to this study is the putative mechanism by which acellular scaffolds promote de novo muscle fiber regeneration. A teleological mechanism is that scaffold-promoted regeneration recapitulates the *normal* spatiotemporal events of muscle fiber repair and regeneration observed after recoverable injuries (Ciciliot and Schiaffino 2010) and for whole muscle regeneration by autologous minced muscle (Ghins et al. 1984; Carlson 1968; Snow 1973; Studitsky 1964). Following recoverable injuries, factors released from injured muscle fibers induce an intricate spatiotemporal communication between the innate immune response and myogenic progenitor cell activity (i.e., primary satellite cells) that promotes repair and regeneration of the injured tissue (Tidball and Villalta 2010). Disruption of either the immune response or satellite cell activity impairs regeneration (Ochoa et al.

2007; Warren et al. 2005; Lepper et al. 2011). Within the defect in close proximity to the remaining musculature, there was evidence that this process was occurring 2 weeks after devitalized graft transplantation, as $Pax7^+$ cells, small regenerating myobfibers, and macrophages were all colocalized (Figs. 4–6). However, beyond no more than 0.5 mm from the remaining muscle mass, no evidence of $Pax7^+$ or $myosin^+$ cells was present in the defect, and no evidence of further regeneration had occurred by 8 weeks post-injury. In contrast, minced graft transplantation presented muscle fiber regeneration throughout the defect with associated satellite cell ($Pax7^+$) colocalization (Figs. 4 and 5), which may have been derived from the transplanted grafts or migrated from the host tissue. As an alternative myogenic cell source, perivascular stem cells and $CD133^+$ progenitors have been identified previously within regenerating muscle fibers in the area where decellularized scaffolds were transplanted (Sicari et al. 2014; Turner et al. 2010). In the current study we also observed that $Sca\text{-}1^+$ cells were prevalent in defect regions not populated by $Pax7^+$ cells after devitalized graft transplantation 2 weeks post-injury (Fig. 5). Sca-1 is expressed on a variety of stem and progenitor cells including, but not limited to, hematopoietic stem cells, muscle-derived stem cells and side population cells (Torrente et al. 2001; Polesskaya et al. 2003; Zammit et al. 2006). Although we did not further identify these $Sca\text{-}1^+$ cells, their presence indicates that stem and progenitor cells are capable of migrating into the devitalized grafts, and further raises the question as to whether these potentially alternative myogenic cells require interaction with adult myofibers or activated satellite cells (Camargo et al. 2003) to induce myogenic function. Based on these findings it appears that de novo muscle fiber regeneration promoted by devitalized and vital scaffolds may be partially dependent on satellite cell activity.

The role of the inflammatory response and the importance of conversion from pro- to an anti-inflammatory phenotype has become an increasingly recognized component in regeneration. Resident and recruited macrophages, among other immune cells, exhibit complex and heterogeneous phenotypes that are believed to be sequentially activated and abated in a timely fashion through the phases of repair and regeneration. Pro-inflammatory activity is important for the migration and activation of myogenic precursor cells (Tidball and Villalta 2010; Arnold et al. 2007; Tidball and Wehling-Henricks 2007), while an anti-inflammatory response stimulates muscle precursor cell differentiation and myotube formation (Brown et al. 2012; Arnold et al. 2007; Tidball and Wehling-Henricks 2007, Tidball and Villalta 2010). In this study, we generally characterized the inflammatory response of muscles repaired with devitalized and vital grafts at 2 weeks post-injury. The expression of CD163, widely recognized as a macrophage specific anti-inflammatory marker (Moestrup and Moller 2004; Van Gorp et al. 2010; Kowal et al. 2011; Raes et al. 2002a, 2002b; Mosser 2003) was significantly lower in devitalized than vital graft-repaired muscles indicating an inferior anti-inflammatory (M2-like) macrophage polarization (Fig. 6). Furthermore, the overall inflammatory response despite the greater presence of CD68+ macrophages in devitalized graft-repaired muscles appeared to be functionally less active since TNF-α, IL-12, IL-4, IL-10, VEGF, and TGF-β1 expression was significantly lower also. Interestingly, since TNF-α is involved in the recruitment, activation, and proliferation of muscle precursor and $pax7^+$ satellite cells (Li 2003; Guttridge et al. 1999), and IL-4 and IL-10 are associated with the differentiation and maturation of myoblasts into myotubes (Arnold et al. 2007; Tidball and Villalta 2010), the lower gene expression of these markers suggests that the inflammatory response to the devitalized grafts is not conducive to continued fiber regeneration in areas further than ~.5 mm from the remaining musculature.

Because several inflammatory cells express surface markers such as CCR7, CD86, FIZZ1, Arginase 1, and MRC1 (Munder et al. 1999, Murphy et al. 2008; Zea et al. 2005; Nair et al. 2005), it is difficult to conclude a specific macrophage phenotype in vivo. Moreover, M1 and M2 are hypothetical ends of a spectrum and macrophages can acquire overlapping phenotypical states that co-express M1 and M2 markers (Kou and Babensee 2010; Biswas and Mantovani 2010). To further understand the effect of devitalized and vital grafts exclusively and specifically on macrophages, an in-vitro study was conducted using bone marrow derived macrophages. The study showed that both devitalized and vital grafts induced a mixed macrophage phenotype response on day 1, but only the vital grafts were able to induce and maintain a more M2-like phenotype by day 4 (Fig. 7). This in vitro study demonstrates that in the absence of biological cues from live and functionally active cells, macrophages do not acquire or maintain a functionally active M2 or pro-regenerative phenotype. Therefore, we postulate that 2 weeks post-injury in vivo the inflammatory cells (e.g., macrophages) in the devitalized grafts (1) have an attenuated functional activity, and (2) the paucity or absence of their biological stimuli diminishes the migration and sustenance of myogenic cells (e.g., Pax $7^+$ satellite cells) in the defect site (Fig. 5a). This speculation is partially supported by the low expression of IL-4, IL-12, IL-10, TNF-α, TGF-β1, and VEGF in the devitalized graft-repaired muscles at 2 weeks post-injury (Fig. 6), but requires further testing in VML models of a clinically relevant scale. An extension of these findings is that functionally active pro- and anti-inflammatory cells (e.g., M1 and M2 macrophage phenotypes) are important for de novo regeneration of VML-injured skeletal muscle. In support of this contention, other studies have also shown that a mixed macrophage phenotype response (consisting of both M1 and M2) is required for scaffold vascularization (Spiller et al. 2014) and remodeling (Agrawal et al. 2012). A prolonged

and unrestrained M1 macrophage response or an early and premature M2 response has been shown to result in aberrant regenerative outcomes (Li 2003; Sindrilaru et al. 2011; Chen et al. 2005; Torrente et al. 2003; Warren et al. 2002). Furthermore, a chronic injury like VML consists of repeated degeneration-regeneration cycles creating a complex cellular microenvironment (Corona et al. 2013a, 2013c). Therefore, coordinated efforts by both pro- and anti-inflammatory cells (e.g., M1 and M2 macrophage phenotypes) might be required for effective regeneration of VML, as demonstrated by the vital grafts in this study.

The functional improvements promoted by transplantation of devitalized grafts are encouraging for the clinical translation of acellular scaffolds. We suggest that the limited fiber regeneration observed with the devitalized grafts, in comparison to that promoted by the vital graft positive control group, is not likely to significantly contribute to functional recovery. However, the fibrotic mass deposited in the defect in response to devitalized grafts, while not itself contractile, also corresponded to a significant (*albeit lesser than vital grafts*) functional improvement compared to no repair (Fig. 2 and 3). We (Corona et al. 2013a) and others (Chen and Walters 2013) have previously observed this *functional fibrosis* using a variety of decellularized scaffolds in rodent VML models. A recent clinical study reported that UBM transplantation improved the functional capacity of individuals with VML (Sicari et al. 2014). Given the low density of small muscle fibers that regenerated in this study, it is plausible that a portion of the functional improvement may have been due to improved force transmission. In this regard, a scaffold designed to constructively model a mechanical bridge in the defect may optimize force transmission and protect the remaining musculature from functional overload (Corona et al. 2013a), and therefore may be an exemplary surgical intervention used for acute repair of VML. That being said, functional recovery of VML-injured muscle will only approach its full potential with restoration of the lost muscle mass. Thus, the goal of emerging therapies should remain focused on functional gains made through regeneration.

Herein, we demonstrate that de novo muscle fiber regeneration in a VML defect following devitalized scaffold transplantation is limited, and restricted to areas in close proximity to the remaining musculature. These findings indicate that transplantation of a devitalized scaffold without local queues from injured skeletal muscle is too great a deviation from the normal spatiotemporal events that define mammalian skeletal muscle regeneration. A stark absence is the presence of satellite cells in remote regions of the defect, and an attenuated activity of pro- and anti-inflammatory cells. As a positive control, vital minced grafts comprised of myogenic and scaffold elements allow for interaction with the ensuing inflammatory response and the promotion of muscle tissue regeneration throughout the defect area. The current results suggest that de novo muscle fiber regeneration promoted by devitalized grafts may be improved if the migration distance for myogenic cells is reduced.

**Acknowledgments** We thank Ms. Janet Roe for her technical assistance. These studies were funded by the Combat Casualty Care Research Program, Medical Research and Materiel Command.

## References

Agrawal H, Tholpady SS, Capito AE, Drake DB, Katz AJ (2012) Macrophage phenotypes correspond with remodeling outcomes of various acellular dermal matrices. Open Access J Regen Med 1:51–59

Arnold L, Henry A, Poron F, Baba-Amer Y, van Rooijen N, Plonquet A, Gherardi RK, Chazaud B (2007) Inflammatory monocytes recruited after skeletal muscle injury switch into antiinflammatory macrophages to support myogenesis. J Exp Med 204:1057–1069

Biswas SK, Mantovani A (2010) Macrophage plasticity and interaction with lymphocyte subsets: cancer as a paradigm. Nat Immunol 11:889–896

Brown BN, Valentin JE, Stewart-Akers AM, McCabe GP, Badylak SF (2009) Macrophage phenotype and remodeling outcomes in response to biologic scaffolds with and without a cellular component. Biomaterials 30:1482–1491

Brown BN, Londono R, Tottey S, Zhang L, Kukla KA, Wolf MT, Daly KA, Reing JE, Badylak SF (2012) Macrophage phenotype as a predictor of constructive remodeling following the implantation of biologically derived surgical mesh materials. Acta Biomater 8:978–987

Camargo FD, Green R, Capetanaki Y, Jackson KA, Goodell MA (2003) Single hematopoietic stem cells generate skeletal muscle through myeloid intermediates. Nat Med 9:1520–1527

Carlson BM (1968) Regeneration of the completely excised gastrocnemius muscle in the frog and rat from minced muscle fragments. J Morphol 125:447–472

Chen XK, Walters TJ (2013) Muscle-derived decellularised extracellular matrix improves functional recovery in a rat latissimus dorsi muscle defect model. J Plast Reconstr Aesthet Surg 66(12):1750–1758

Chen SE, Gerken E, Zhang Y, Zhan M, Mohan RK, Li AS, Reid MB, Li YP (2005) Role of TNF-{alpha} signaling in regeneration of cardiotoxin-injured muscle. Am J Physiol Cell Physiol 289:C1179–C1187

Ciciliot S, Schiaffino S (2010) Regeneration of mammalian skeletal muscle. Basic Mech Clin Implications Curr Pharm Des 16:906–914

Corona BT, Machingal MA, Criswell T, Vadhavkar M, Dannahower AC, Bergman C, Zhao W, Christ GJ (2012) Further development of a tissue engineered muscle repair construct in vitro for enhanced functional recovery following implantation in vivo in a murine model of volumetric muscle loss injury. Tissue Eng Part A 18:1213–1228

Corona BT, Wu X, Ward CL, McDaniel JS, Rathbone CR, Walters TJ (2013a) The promotion of a functional fibrosis in skeletal muscle with volumetric muscle loss injury following the transplantation of muscle-ECM. Biomaterials 343:3324–3335

Corona BT, Ward CL, Baker HB, Walters TJ, Christ GJ (2013b) Implantation of in vitro tissue engineered muscle repair constructs and bladder acellular matrices partially restore in vivo skeletal muscle function in a rat model of volumetric muscle loss injury. Tissue Eng Part A 20:705–715

Corona BT, Garg K, Ward CL, McDaniel JS, Walters TJ, Rathbone CR (2013c) Autologous minced muscle grafts: a tissue engineering

therapy for the volumetric loss of skeletal muscle. Am J Physiol Cell Physiol 305:C761–775
Corso P, Finkelstein E, Miller T, Fiebelkorn I, Zaloshnja E (2006) Incidence and lifetime costs of injuries in the United States. Inj Prev J Int Soc Child Adolesc Inj Prev 12:212–218
Gamba PG, Conconi MT, Lo Piccolo R, Zara G, Spinazzi R, Parnigotto PP (2002) Experimental abdominal wall defect repaired with acellular matrix. Pediatr Surg Int 18:327–331
Garg K, Pullen NA, Oskeritzian CA, Ryan JJ, Bowlin GL (2013) Macrophage functional polarization (M1/M2) in response to varying fiber and pore dimensions of electrospun scaffolds. Biomaterials 34: 4439–4451
Ghins E, Colson-van Schoor M, Marechal G (1984) The origin of muscle stem cells in rat triceps surae regenerating after mincing. J Muscle Res Cell Motil 5:711–722
Ghins E, Colson-Van Schoor M, Maldague P, Marechal G (1985) Muscle regeneration induced by cells autografted in adult rats. Arch Int Physiol Biochim 93:143–153
Ghins E, Colson-Van Schoor M, Marechal G (1986) Implantation of autologous cells in minced and devitalized rat skeletal muscles. J Muscle Res Cell Motil 7:151–159
Grogan BF, Hsu JR (2011) Volumetric muscle loss. J Am Acad Orthop Surg 19(Suppl 1):S35–37
Guttridge DC, Albanese C, Reuther JY, Pestell RG, Baldwin AS Jr (1999) NF-kappaB controls cell growth and differentiation through transcriptional regulation of cyclin D1. Mol Cell Biol 19:5785–5799
Huijing PA, Jaspers RT (2005) Adaptation of muscle size and myofascial force transmission: a review and some new experimental results. Scand J Med Sci Sports 15:349–380
Keane TJ, Badylak SF (2014) The host response to allogeneic and xenogeneic biological scaffold materials. J Tissue Eng Regen Med Feb 14 [Epub ahead of print]
Kou PM, Babensee JE (2010) Macrophage and dendritic cell phenotypic diversity in the context of biomaterials. J Biomed Mater Res A 96: 239–260
Kowal K, Silver R, Slawinska E, Bielecki M, Chyczewski L, Kowal-Bielecka O (2011) CD163 and its role in inflammation. Folia Histochem Cytobiol 49:365–374
Lee JM, Pereira CA, Abdulla D, Naimark WA, Crawford I (1995) A multi-sample denaturation temperature tester for collagenous biomaterials. Med Eng Phys 17:115–121
Lepper C, Partridge TA, Fan CM (2011) An absolute requirement for Pax7-positive satellite cells in acute injury-induced skeletal muscle regeneration. Development 138:3639–3646
Li YP (2003) TNF-alpha is a mitogen in skeletal muscle. Am J Physiol Cell Physiol 285:C370–376
Liao J, Joyce EM, Sacks MS (2008) Effects of decellularization on the mechanical and structural properties of the porcine aortic valve leaflet. Biomaterials 29:1065–1074
Lu H, Hoshiba T, Kawazoe N, Chen G (2011) Autologous extracellular matrix scaffolds for tissue engineering. Biomaterials 32:2489–2499
Machingal MA, Corona BT, Walters TJ, Kesireddy V, Koval CN, Dannahower A, Zhao W, Yoo JJ, Christ GJ (2011) A tissue-engineered muscle repair construct for functional restoration of an irrecoverable muscle injury in a murine model. Tissue Eng Part A 17:2291–2303
Mase VJ Jr, Hsu JR, Wolf SE, Wenke JC, Baer DG, Owens J, Badylak SF, Walters TJ (2010) Clinical application of an acellular biologic scaffold for surgical repair of a large, traumatic quadriceps femoris muscle defect. Orthopedics 33:511
Merritt EK, Hammers DW, Tierney M, Suggs LJ, Walters TJ, Farrar RP (2010a) Functional assessment of skeletal muscle regeneration utilizing homologous extracellular matrix as scaffolding. Tissue Eng Part A 16:1395–1405
Merritt EK, Cannon MV, Hammers DW, Le LN, Gokhale R, Sarathy A, Song TJ, Tierney MT, Suggs LJ, Walters TJ, Farrar RP (2010b) Repair of traumatic skeletal muscle injury with bone-marrow-derived mesenchymal stem cells seeded on extracellular matrix. Tissue Eng Part A 16:2871–2881
Miles CA, Ghelashvili M (1999) Polymer-in-a-box mechanism for the thermal stabilization of collagen molecules in fibers. Biophys J 76: 3243–3252
Moestrup SK, Moller HJ (2004) CD163: a regulated hemoglobin scavenger receptor with a role in the anti-inflammatory response. Ann Med 36:347–354
Morgan JE, Coulton GR, Partridge TA (1987) Muscle precursor cells invade and repopulate freeze-killed muscles. J Muscle Res Cell Motil 8:386–396
Mosser DM (2003) The many faces of macrophage activation. J Leukoc Biol 73:209–212
Munder M, Eichmann K, Modolell M (1998) Alternative metabolic states in murine macrophages reflected by the nitric oxide synthase/arginase balance: competitive regulation by CD4+ T cells correlates with Th1/Th2 phenotype. J Immunol 160:5347–5354
Munder M, Eichmann K, Moran JM, Centeno F, Soler G, Modolell M (1999) Th1/Th2-regulated expression of arginase isoforms in murine macrophages and dendritic cells. J Immunol 163:3771–3777
Murphy K, Paul T, Walport M (2008) Janeway's immunobiology. Garland Science, Taylor and Francis Group, LLC
Nair MG, Gallagher IJ, Taylor MD, Loke P, Coulson PS, Wilson RA, Maizels RM, Allen JE (2005) Chitinase and Fizz family members are a generalized feature of nematode infection with selective up-regulation of Ym1 and Fizz1 by antigen-presenting cells. Infect Immun 73:385–394
Ochoa O, Sun D, Reyes-Reyna SM, Waite LL, Michalek JE, McManus LM, Shireman PK (2007) Delayed angiogenesis and VEGF production in CCR2−/− mice during impaired skeletal muscle regeneration. Am J Physiol Regul Integr Comp Physiol 293:R651–R661
Owens BD, Kragh JF Jr, Macaitis J, Svoboda SJ, Wenke JC (2007) Characterization of extremity wounds in operation iraqi freedom and operation enduring freedom. J Orthop Trauma 21:254–257
Owens BD, Kragh JF Jr, Wenke JC, Macaitis J, Wade CE, Holcomb JB (2008) Combat wounds in operation Iraqi Freedom and operation Enduring Freedom. J Trauma 64:295–299
Polesskaya A, Seale P, Rudnicki MA (2003) Wnt signaling induces the myogenic specification of resident CD45+ adult stem cells during muscle regeneration. Cell 113:841–852
Raes G, De Baetselier P, Noel W, Beschin A, Brombacher F, Hassanzadeh Gh G (2002a) Differential expression of FIZZ1 and Ym1 in alternatively versus classically activated macrophages. J Leukoc Biol 71: 597–602
Raes G, Noel W, Beschin A, Brys L, de Baetselier P, Hassanzadeh GH (2002b) FIZZ1 and Ym as tools to discriminate between differentially activated macrophages. Dev Immunol 9:151–159
Rossi CA, Flaibani M, Blaauw B, Pozzobon M, Figallo E, Reggiani C, Vitiello L, Elvassore N, De Coppi P (2011) In vivo tissue engineering of functional skeletal muscle by freshly isolated satellite cells embedded in a photopolymerizable hydrogel. FASEB J 25:2296–2304
Schenke-Layland K, Vasilevski O, Opitz F, Konig K, Riemann I, Halbhuber KJ, Wahlers T, Stock UA (2003) Impact of decellularization of xenogeneic tissue on extracellular matrix integrity for tissue engineering of heart valves. J Struct Biol 143:201–208
Schultz E, Jaryszak DL, Valliere CR (1985) Response of satellite cells to focal skeletal muscle injury. Muscle Nerve 8:217–222
Schultz E, Jaryszak DL, Gibson MC, Albright DJ (1986) Absence of exogenous satellite cell contribution to regeneration of frozen skeletal muscle. J Muscle Res Cell Motil 7:361–367
Seif-Naraghi SB, Salvatore MA, Schup-Magoffin PJ, Hu DP, Christman KL (2010) Design and characterization of an injectable pericardial matrix gel: a potentially autologous scaffold for cardiac tissue engineering. Tissue Eng Part A 16:2017–2027

Sicari BM, Rubin JP, Dearth CL, Wolf MT, Ambrosio F, Boninger M, Turner NJ, Weber DJ, Simpson TW, Wyse A, Brown EHP, Dziki JL, Fisher LE, Brown S, Badylak SF (2014) An acellular biologic scaffold promotes skeletal muscle formation in mice and humans with volumetric muscle loss. Science Transl Med 6:234ra58

Siegel AL, Atchison K, Fisher KE, Davis GE, Cornelison DD (2009) 3D timelapse analysis of muscle satellite cell motility. Stem Cells 27: 2527–2538

Sindrilaru A, Peters T, Wieschalka S, Baican C, Baican A, Peter H, Hainzl A, Schatz S, Qi Y, Schlecht A, Weiss JM, Wlaschek M, Sunderkotter C, Scharffetter-Kochanek K (2011) An unrestrained proinflammatory M1 macrophage population induced by iron impairs wound healing in humans and mice. J Clin Invest 121:985–997

Snow MH (1973) Metabolic activity during the degenerative and early regenerative stages of minced skeletal muscle. Anat Rec 176:185–203

Spiller KL, Anfang RR, Spiller KJ, Ng J, Nakazawa KR, Daulton JW, Vunjak-Novakovic G (2014) The role of macrophage phenotype in vascularization of tissue engineering scaffolds. Biomaterials 35: 4477–4488

Studitsky AN (1964) Free auto- and homografts of muscle tissue in experiments on animals. Ann N Y Acad Sci 120:789–801

Tidball JG, Villalta SA (2010) Regulatory interactions between muscle and the immune system during muscle regeneration. Am J Physiol Regul Integr Comp Physiol 298:R1173–1187

Tidball JG, Wehling-Henricks M (2007) Macrophages promote muscle membrane repair and muscle fibre growth and regeneration during modified muscle loading in mice in vivo. J Physiol 578:327–336

Torrente Y, Tremblay JP, Pisati F, Belicchi M, Rossi B, Sironi M, Fortunato F, El Fahime M, D'Angelo MG, Caron NJ, Constantin G, Paulin D, Scarlato G, Bresolin N (2001) Intraarterial injection of muscle-derived CD34(+)Sca-1(+) stem cells restores dystrophin in mdx mice. J Cell Biol 152:335–348

Torrente Y, El Fahime E, Caron NJ, Del Bo R, Belicchi M, Pisati F, Tremblay JP, Bresolin N (2003) Tumor necrosis factor-alpha (TNF-alpha) stimulates chemotactic response in mouse myogenic cells. Cell Transplant 12:91–100

Turner NJ, Yates AJ Jr, Weber DJ, Qureshi IR, Stolz DB, Gilbert TW, Badylak SF (2010) Xenogeneic extracellular matrix as an inductive scaffold for regeneration of a functioning musculotendinous junction. Tissue Eng Part A 16:3309–3317

Turner NJ, Badylak JS, Weber DJ, Badylak SF (2012) Biologic scaffold remodeling in a dog model of complex musculoskeletal injury. J Surg Res 176:490–502

Valentin JE, Turner NJ, Gilbert TW, Badylak SF (2010) Functional skeletal muscle formation with a biologic scaffold. Biomaterials 31:7475–7484

Van Gorp H, Delputte PL, Nauwynck HJ (2010) Scavenger receptor CD163, a Jack-of-all-trades and potential target for cell-directed therapy. Mol Immunol 47:1650–1660

Vos T, Flaxman AD, Naghavi M, Lozano R, Michaud C, Ezzati M, Shibuya K, Salomon JA, Abdalla S, Aboyans V, Abraham J, Ackerman I, Aggarwal R, Ahn SY, Ali MK, Alvarado M, Anderson HR, Anderson LM, Andrews KG, Atkinson C, Baddour LM, Bahalim AN, Barker-Collo S, Barrero LH, Bartels DH, Basanez MG, Baxter A, Bell ML, Benjamin EJ, Bennett D, Bernabe E, Bhalla K, Bhandari B, Bikbov B, Bin Abdulhak A, Birbeck G, Black JA, Blencowe H, Blore JD, Blyth F, Bolliger I, Bonaventure A, Boufous S, Bourne R, Boussinesq M, Braithwaite T, Brayne C, Bridgett L, Brooker S, Brooks P, Brugha TS, Bryan-Hancock C, Bucello C, Buchbinder R, Buckle G, Budke CM, Burch M, Burney P, Burstein R, Calabria B, Campbell B, Canter CE, Carabin H, Carapetis J, Carmona L, Cella C, Charlson F, Chen H, Cheng AT, Chou D, Chugh SS, Coffeng LE, Colan SD, Colquhoun S, Colson KE, Condon J, Connor MD, Cooper LT, Corriere M, Cortinovis M, de Vaccaro KC, Couser W, Cowie BC, Criqui MH, Cross M, Dabhadkar KC, Dahiya M, Dahodwala N, Damsere-Derry J, Danaei G, Davis A, De Leo D, Degenhardt L, Dellavalle R, Delossantos A, Denenberg J, Derrett S, Des Jarlais DC, Dharmaratne SD, Dherani M, Diaz-Torne C, Dolk H, Dorsey ER, Driscoll T, Duber H, Ebel B, Edmond K, Elbaz A, Ali SE, Erskine H, Erwin PJ, Espindola P, Ewoigbokhan SE, Farzadfar F, Feigin V, Felson DT, Ferrari A, Ferri CP, Fevre EM, Finucane MM, Flaxman S, Flood L, Foreman K, Forouzanfar MH, Fowkes FG, Franklin R, Fransen M, Freeman MK, Gabbe BJ, Gabriel SE, Gakidou E, Ganatra HA, Garcia B, Gaspari F, Gillum RF, Gmel G, Gosselin R, Grainger R, Groeger J, Guillemin F, Gunnell D, Gupta R, Haagsma J, Hagan H, Halasa YA, Hall W, Haring D, Haro JM, Harrison JE, Havmoeller R, Hay RJ, Higashi H, Hill C, Hoen B, Hoffman H, Hotez PJ, Hoy D, Huang JJ, Ibeanusi SE, Jacobsen KH, James SL, Jarvis D, Jasrasaria R, Jayaraman S, Johns N, Jonas JB, Karthikeyan G, Kassebaum N, Kawakami N, Keren A, Khoo JP, King CH, Knowlton LM, Kobusingye O, Koranteng A, Krishnamurthi R, Lalloo R, Laslett LL, Lathlean T, Leasher JL, Lee YY, Leigh J, Lim SS, Limb E, Lin JK, Lipnick M, Lipshultz SE, Liu W, Loane M, Ohno SL, Lyons R, Ma J, Mabweijano J, MacIntyre MF, Malekzadeh R, Mallinger L, Manivannan S, Marcenes W, March L, Margolis DJ, Marks GB, Marks R, Matsumori A, Matzopoulos R, Mayosi BM, McAnulty JH, McDermott MM, McGill N, McGrath J, Medina-Mora ME, Meltzer M, Mensah GA, Merriman TR, Meyer AC, Miglioli V, Miller M, Miller TR, Mitchell PB, Mocumbi AO, Moffitt TE, Mokdad AA, Monasta L, Montico M, Moradi-Lakeh M, Moran A, Morawska L, Mori R, Murdoch ME, Mwaniki MK, Naidoo K, Nair MN, Naldi L, Narayan KM, Nelson PK, Nelson RG, Nevitt MC, Newton CR, Nolte S, Norman P, Norman R, O'Donnell M, O'Hanlon S, Olives C, Omer SB, Ortblad K, Osborne R, Ozgediz D, Page A, Pahari B, Pandian JD, Rivero AP, Patten SB, Pearce N, Padilla RP, Perez-Ruiz F, Perico N, Pesudovs K, Phillips D, Phillips MR, Pierce K, Pion S, Polanczyk GV, Polinder S, Pope CA, 3rd Popova S, Porrini E, Pourmalek F, Prince M, Pullan RL, Ramaiah KD, Ranganathan D, Razavi H, Regan M, Rehm JT, Rein DB, Remuzzi G, Richardson K, Rivara FP, Roberts T, Robinson C, De Leon FR, Ronfani L, Room R, Rosenfeld LC, Rushton L, Sacco RL, Saha S, Sampson U, Sanchez-Riera L, Sanman E, Schwebel DC, Scott JG, Segui-Gomez M, Shahraz S, Shepard DS, Shin H, Shivakoti R, Singh D, Singh GM, Singh JA, Singleton J, Sleet DA, Sliwa K, Smith E, Smith JL, Stapelberg NJ, Steer A, Steiner T, Stolk WA, Stovner LJ, Sudfeld C, Syed S, Tamburlini G, Tavakkoli M, Taylor HR, Taylor JA, Taylor WJ, Thomas B, Thomson WM, Thurston GD, Tleyjeh IM, Tonelli M, Towbin JA, Truelsen T, Tsilimbaris MK, Ubeda C, Undurraga EA, van der Werf MJ, van Os J, Vavilala MS, Venketasubramanian N, Wang M, Wang W, Watt K, Weatherall DJ, Weinstock MA, Weintraub R, Weisskopf MG, Weissman MM, White RA, Whiteford H, Wiersma ST, Wilkinson JD, Williams HC, Williams SR, Witt E, Wolfe F, Woolf AD, Wulf S, Yeh PH, Zaidi AK, Zheng ZJ, Zonies D, Lopez AD, Murray CJ, AlMazroa MA, Memish ZA (2012) Years lived with disability (YLDs) for 1160 sequelae of 289 diseases and injuries 1990–2010: a systematic analysis for the Global Burden of Disease Study 2010. Lancet 380:2163–2196

Warren GL, Hulderman T, Jensen N, McKinstry M, Mishra M, Luster MI, Simeonova PP (2002) Physiological role of tumor necrosis factor alpha in traumatic muscle injury. FASEB J 16:1630–1632

Warren GL, Hulderman T, Mishra D, Gao X, Millecchia L, O'Farrell L, Kuziel WA, Simeonova PP (2005) Chemokine receptor CCR2 involvement in skeletal muscle regeneration. FASEB J 19:413–415

Williams C, Liao J, Joyce EM, Wang B, Leach JB, Sacks MS, Wong JY (2009) Altered structural and mechanical properties in decellularized rabbit carotid arteries. Acta Biomater 5:993–1005

Wolf MT, Daly KA, Reing JE, Badylak SF (2012) Biologic scaffold composed of skeletal muscle extracellular matrix. Biomaterials 33: 2916–2925

Wu X, Corona BT, Chen X, Walters TJ (2012a) A standardized rat model of volumetric muscle loss injury for the development of tissue engineering therapies. Biores Open Access 1:280–290

Zammit PS, Partridge TA, Yablonka-Reuveni Z (2006) The skeletal muscle satellite cell: the stem cell that came in from the cold. J Histochem Cytochem Off J Histochem Soc 54:1177–1191

Zea AH, Rodriguez PC, Atkins MB, Hernandez C, Signoretti S, Zabaleta J, McDermott D, Quiceno D, Youmans A, O'Neill A, Mier J, Ochoa AC (2005) Arginase-producing myeloid suppressor cells in renal cell carcinoma patients: a mechanism of tumor evasion. Cancer Res 65:3044–3048

Zheng MH, Chen J, Kirilak Y, Willers C, Xu J, Wood D (2005) Porcine small intestine submucosa (SIS) is not an acellular collagenous matrix and contains porcine DNA: possible implications in human implantation. J Biomed Mater Res B Appl Biomater 73B:61–67